Energy loss of 0.7-MeV He ions due to the dynamic response of surface electrons

Yoshikazu Fujii, Keiji Kishine, Kazumasa Narumi, Kenji Kimura, and Michi-hiko Mannami
Department of Engineering Science, Kyoto University, Kyoto 606-01, Japan
(Received 16 June 1992)

The energy losses of 0.7-MeV He ions which have surface channeled along atomic rows on a clean (100) surface of SnTe are studied. An energy spectrum of the surface-channeled ions shows a few peaks whose energies and heights depend on the angle of incidence of He ions, θ_i. From the θ_i dependence of the energy losses, position-dependent stopping powers of the (100) surface for the He ions are determined at the [001] and [011] surface channeling. The contribution of collective excitation of surface valence electrons to the stopping powers is extracted from the obtained position-dependent stopping powers. This agrees well with the theories where the dynamical response of valence electrons to the fast-moving ions is taken into account.

PACS number(s): 34.50.Bw, 61.80.Mk

I. INTRODUCTION

Using glancing-angle scattering of mega-electron-volt ions from a flat crystal surface, it has been shown that the ion loses kinetic energy even if it travels outside the solid [1,2]. The energy losses of the ions have been explained by a position-dependent stopping power of the (100) surface of SnTe for fast ions in vacuum. The stopping power has a form [1],

$$S^{100}(x)=CE^{-1/2}\exp\left[-\beta_3\frac{x}{2a_{\mathrm{TF}}}\right], \quad (1)$$

where x is the distance of the ion from the surface atomic plane, C is a constant depending on the ion species and target surface, E is the ion energy, β_3 is 0.3, and a_{TF} is the Thomas-Fermi screening distance. The stopping powers are explained in terms of the deceleration in the field induced by collective excitation of valence electrons to the charge of the fast-moving ion near the surface, and of the collisions of the ion with electrons exuding out of the surface.

The trajectories of the specularly reflected ions can be obtained by applying the general principles of the interaction of a fast ion with orderly arranged atoms developed for ion channeling in crystal [3,4]. Thus the losses of energy of the specularly reflected ions are obtained by integrating the position-dependent stopping power along ion trajectories.

Recently we have proposed a new method to derive position-dependent stopping power of a surface for specularly reflected ions at glancing-angle incidence on the surface [2]. With this method, the position-dependent stopping power was derived experimentally only from the dependence of the energy loss ΔE of ions on the angle of incidence on the surface. In the present paper, we apply this method for the analysis of the energy losses of surface-channeled He ions at the (100) surface of SnTe. Then the position-dependent stopping powers of the (100) surface for 0.7-MeV He ions at the [001] and [011] surface channeling are determined. Contribution of the collective excitation of surface valence electrons to the stopping powers is extracted from the obtained position-dependent stopping powers for surface-channeling ions, which can be compared with those derived from the theories.

II. EXPERIMENT

A single crystal of SnTe with a clean (100) surface was grown expitaxially by vacuum evaporation of SnTe (99.999% purity) on the (100) surface of KCl mounted on a five-axis goniometer in a UHV scattering chamber. The (100) surface of the grown SnTe crystal was irradiated by a narrow beam of 0.7-MeV He^+ ions from the 4-MV Van de Graaff accelerator of Kyoto University. The beam was less than 0.04 mm in diameter and the beam divergence was less than 0.1 mrad at the target position. The SnTe crystals were grown with growth rates less than 0.5 nm/min at 250 °C. At these growth rates the densities of steps on the (100) surfaces were small, which was ascertained directly by the observation with the use of an atomic-force microscope [5]. Thus the fraction of He ions penetrating the surface at the steps was negligible. The base pressure of the UHV scattering chamber was 3×10^{-10} Torr. The vacuum of the chamber during the epitaxial growth was better than 2×10^{-9} Torr and was in the 10^{-10}-Torr range during the ion-scattering measurement.

Figure 1 shows the angular distribution of scattered He ions which are observed on a fluorescence screen downstream from the crystal when 0.7-MeV He^+ ions scatter at glancing-angle incidence on the (100) surface of SnTe with various azimuthal angles ϕ_i of the incident beam relative to the [011] atomic rows. At the incidence of ions nearly parallel to low-index atomic rows on a crystal surface, the ions are scattered on a broad arc as can be seen in Figs. 1(a)–1(c). The arc is formed by the ions scattered from the atomic rows, and thus the center of the arc is the projection of the direction of the atomic rows on the screen. The arc moves as the direction of the rows deviates from the incident-beam direction.

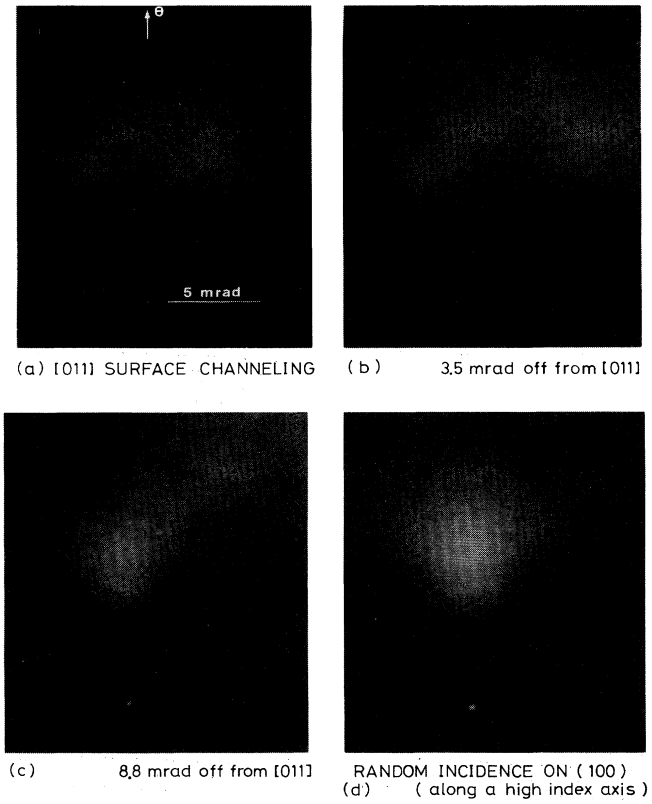

FIG. 1. Angular distributions of scattered He ions at the [011] surface channeling on the (100) surface of SnTe crystal at the incidence of 0.7-MeV He^+ ions. The glancing angle of the incident ions to the (100) surface was 4.8 mrad and the azimuthal angles in the figure were measured from the [011] axis parallel to the (100) surface of SnTe.

An aperture was placed to select the ions scattered at the angle for specular reflection, i.e., at the scattering angle θ twice the angle of incidence θ_i in the scattering plane. The acceptance angle of the aperture was 0.6 mrad. The ions passing through the aperture were energy analyzed with a magnetic spectrometer. Energy resolution of the spectrometer was 8×10^{-3}. Fractions of He^{2+} and He^+ in the scattered ions at 0.7-MeV He^+ incidence are about 0.7 and 0.3, respectively, and He^0 fraction was less than 10^{-2}. The charge of He ion changes so frequently along its trajectory [6] that the energy spectrum of He^+ is almost equal to that of He^{2+}. Thus we studied the energy losses of scattered He^{2+} ions at the [001] and [011] surface channeling.

III. RESULTS AND DISCUSSION

Figures 2 and 3 show the examples of the observed energy spectra of the [001] and [011] surface-channeled He^{2+} ions at the incidence of 0.7-MeV He^+ ions on the (100) surface of SnTe with azimuthal angle $\phi_i=0$. Most of the spectra show a sharp peak at the energies about 15 keV smaller than that of the incident ions. The energy at the highest-energy peak little depend on the angle of incidence as shown in Fig. 4. On the other hand, the ener-

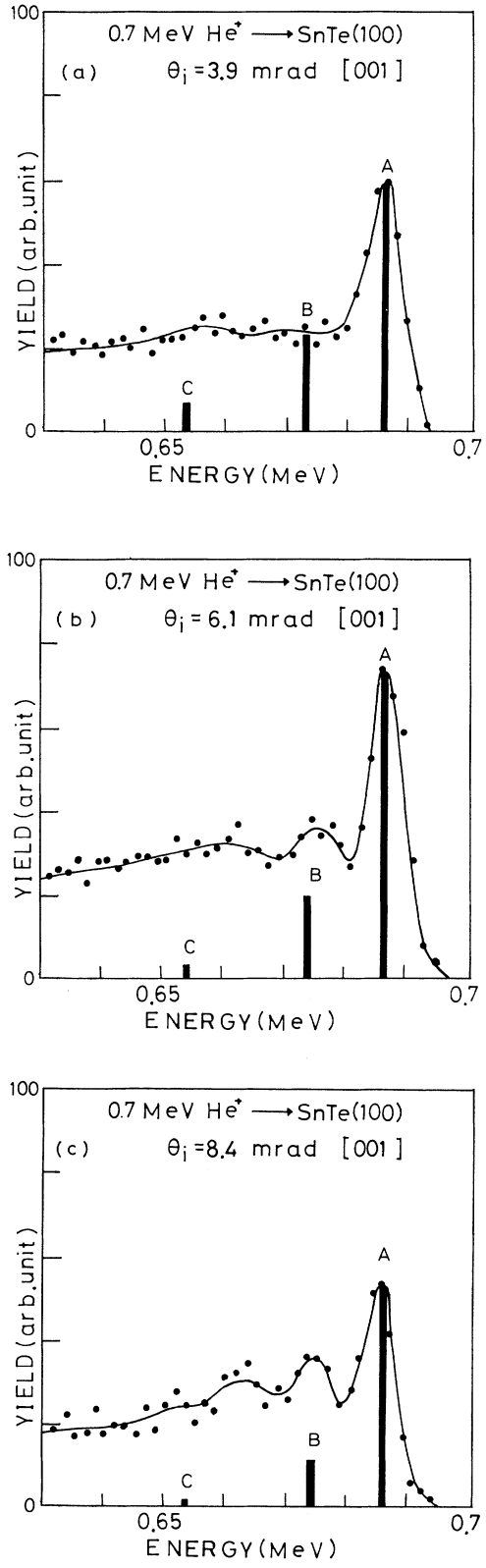

FIG. 2. Energy spectra of the [001] surface-channeled He^{2+} ions at the incidence of 0.7-MeV He^+ ions on the (100) surface of SnTe. (a) $\theta_i=3.9$ mrad. (b) $\theta_i=6.1$ mrad. (c) $\theta_i=8.4$ mrad. The calculated yields at the peaks are shown by bars.

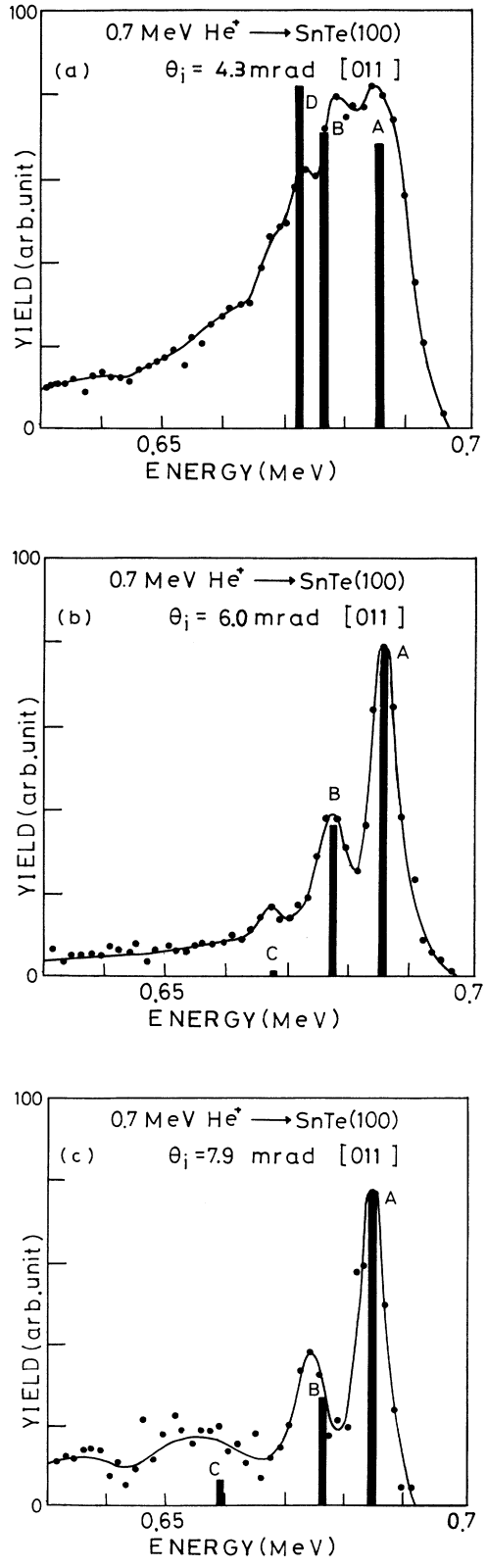

FIG. 3. Energy spectra of the [011] surface-channeled He^{2+} ions at the incidence of 0.7-MeV He^{+} ions on the (100) surface of SnTe. (a) $\theta_i = 4.3$ mrad. (b) $\theta_i = 6.0$ mrad. (c) $\theta_i = 7.9$ mrad. The calculated yields at the peaks are shown by bars.

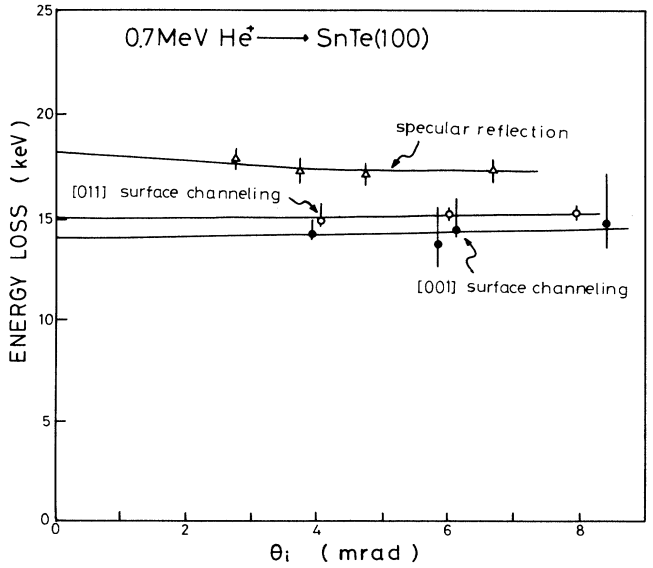

FIG. 4. Dependence of the energy loss at the highest-energy peak in the energy spectra of surface channeled He^{2+} on the angle of incidence. The energy losses at specular reflection from the (100) surface are shown for comparison.

gies at the lower-energy peaks depend on the angle of incidence.

A. Position-dependent stopping powers of atomic rows

For a fast ion of energy E traveling in vacuum nearly parallel to the $[0kl]$ atomic rows on the (100) surface of SnTe crystal, we choose the Cartesian coordinates where the z axis is parallel to the atomic rows and the x axis parallel to the surface normal. The origin of the coordinates is on an atom on the surface. Since the velocity of the ion parallel to the z axis is approximately constant, the equation of motion of the ion projected on the xy plane is written as

$$M\frac{d^2\mathbf{R}}{dt^2} = -\nabla_{x,y} U(\mathbf{R}) , \tag{2}$$

where M is the mass of the ion, $\mathbf{R}$ is the position of the ion projected on the xy plane, and $U(\mathbf{R})$ is the potential for the ion. With the use of the continuum row potential $U_a^{[0kl]}(r)$ of the $[0kl]$ atomic row, where r is the distance from the row [3], the potential $U(\mathbf{R})$ is expressed as

$$U^{[0kl]}(x,y) = \sum_{n=-\infty}^{\infty} U_a^{[0kl]}\{[x^2+(y+na_{[0kl]})^2]^{1/2}\} , \tag{3}$$

where $a_{[0kl]}$ is the distance between the $[0kl]$ atomic rows on the surface.

The potential distributions $U^{[0kl]}(x,y)$ for a fast He ion traveling along the [001] and [011] atomic rows on the (100) surface of SnTe are shown in Fig. 5. Continuum surface planar potential of the (100) surface for He ions is also shown for comparison. The Molière approximation to Thomas-Fermi screening function was used in the calculation of the potentials.

In order to explain the peaks in the energy spectra of

the surface-channeled He ions such as those shown in Figs. 2 and 3, trajectories of He ions were calculated with the use of Eqs. (2) and (3), where the azimuthal angle of the incidence He^+ ions to the atomic row is zero. The trajectory depends on the angle of incidence θ_i and the impact parameter y of the ion–atomic-row collision. Figure 6 shows two examples of the impact-parameter dependence of the angle α of scattering for the [011] surface-channeled 0.7-MeV He ions. The ordinate shows the direction of motion of the scattered ion relative to the scattering plane, which is schematically shown in the inset, and the abscissa shows the impact parameter of the ion–atomic-row collision. The angles for the ion which have penetrated the surface are not shown. When the angle α is zero, the ion is reflected at the angle for specular reflection. It is seen from Figs. 6(a) and (b) that four types of trajectories, shown by A, B, C, and D, give rise to the specular reflection. These trajectories are shown in Fig. 5, where they are projected on the xy plane.

Since the type-A trajectory occurs at any angle θ_i of incidence, it is expected that the highest-energy peaks in the energy spectra shown in Fig. 4 are formed by the ions with the type-A trajectories. It is assumed that the trajectory of type-A is governed only by an $[0kl]$ atomic

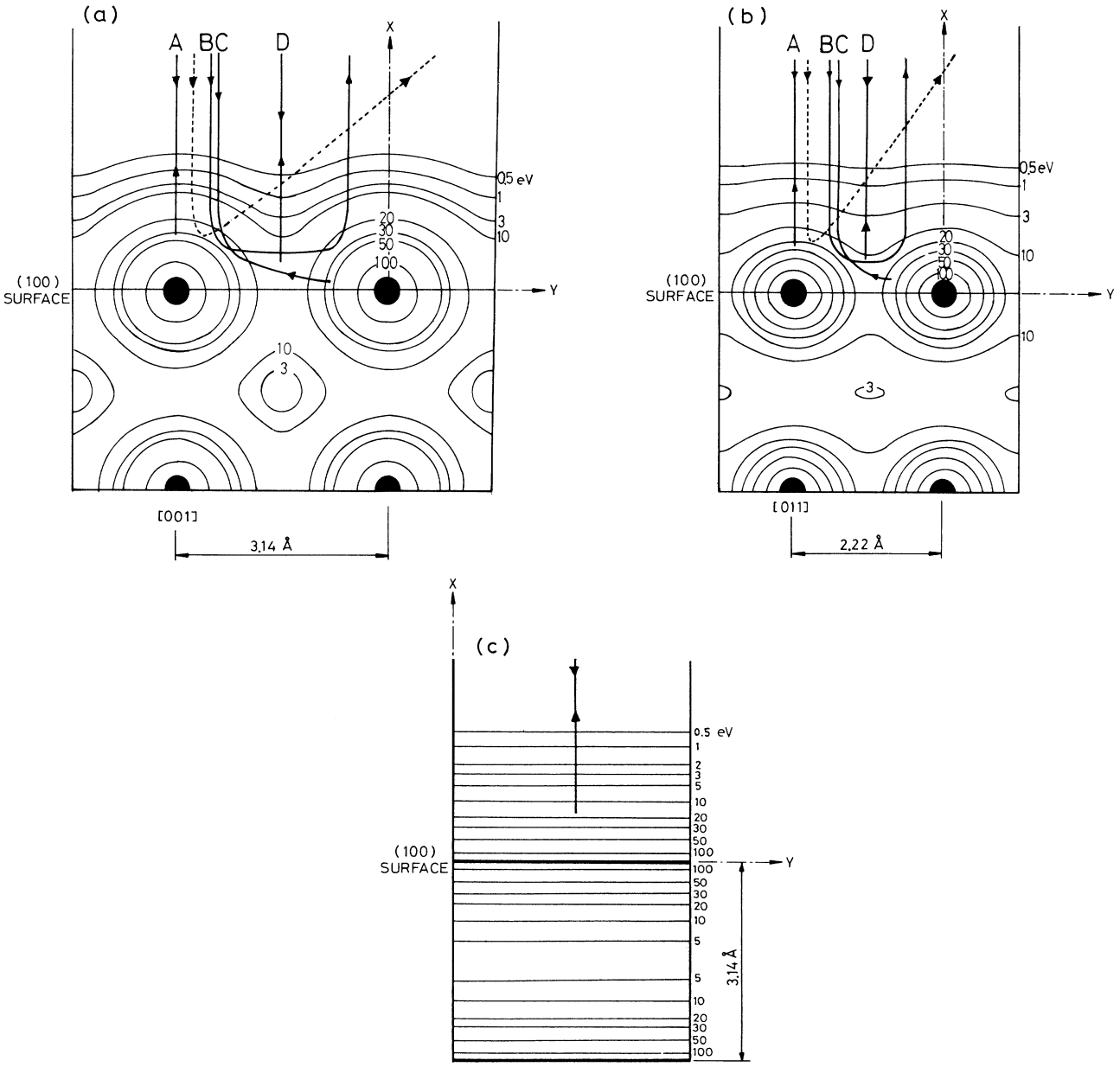

FIG. 5. Potential distributions $U(x,y)$ (contours labeled in eV) for a fast He ion at glancing-angle incidence of the (100) surface of SnTe. (a) Along the [001] axis. (b) Along the [011] axis. (c) Along the high-index axis, the continuum surface planar potential of the (100) surface. Possible trajectories of 0.7-MeV He ions which give rise to the specularly reflected ions at $\theta=2\theta_i$ are shown.

row on the scattering plane, since the trajectory is in the xz plane containing the $[0kl]$ atomic row. Thus the trajectory of the ion is described by the differential equation,

$$\frac{dx}{dz}=\left[\frac{U_a^{[0kl]}(x_c)-U_a^{[0kl]}(x)}{E}\right]^{1/2}, \tag{4}$$

where x_c is the distance of the closest approach of the ion to the atomic row and is thus given by $U_a^{[0kl]}(x_c)=E\theta_i^2$. If the energy loss of the ion is determined by the stopping power which depends on the distance from the $[0kl]$ atomic row, the energy loss $\Delta E(\theta_i)$ of the ions along the type-A trajectories is given by

$$\Delta E(\theta_i)=\int_{\text{traj}} S_a^{[0kl]}(x)dz$$

$$=2\sqrt{E}\int_{x_c}^{\infty}dx\frac{S_a^{[0kl]}(x)}{[U_a^{[0kl]}(x_c)-U_a^{[0kl]}(x)]^{1/2}}, \tag{5}$$

where x is the distance from the surface and $S_a^{[0kl]}(x)$ is the position-dependent stopping power of the $[0kl]$ atomic row for ions with the type-A trajectory. It is only $S_a^{[0kl]}(x)$ that is unknown in Eq. (5), and thus Eq. (5) is an integral equation of the Abel type for $S_a^{[0kl]}(x)$, which is solved as

$$S_a^{[0kl]}(x)=-\frac{1}{2\pi E}\frac{dU_{a(x)}^{[0kl]}}{dx}\left\{\left[\frac{E[\Delta E(0)]^2}{U_a^{[0kl]}(x)}\right]^{1/2}+\int_0^{\pi/2}du\ \Delta E'\left[\left[\frac{U_a^{[0kl]}(x)}{E}\right]^{1/2}\sin u\right]\right\}, \tag{6}$$

where a prime denotes differentiation.

Extrapolating the observed energy loss $\Delta E(\theta_i)$ to $\theta_i=0$ in Fig. 4, and substituting the $\Delta E(\theta_i)$ and $U_a^{[0kl]}(x)$ into Eq. (6), we obtain the stopping powers, $S_a^{[001]}(x)$ and $S_a^{[011]}(x)$ of the (100) surface of SnTe, for the [001] and [011] surface-channeling 0.7-MeV He ions. The same procedure was repeated for the energy losses at the incidence along the random orientation and the stopping power $S^{(100)}(x)$ of the (100) surface for specular reflection was also obtained. The results are shown by solid lines in Fig. 7. The stopping powers $S_a^{[001]}(x)$ and $S_a^{[011]}(x)$ are decreasing functions of x, and are almost equal.

B. Contribution of valence electrons to the stopping powers

It is known that the stopping of fast charged particles in matter is determined by ion-electron single collisions and by the collective response of valence electrons to the moving charge. It is possible to derive the contribution of the collective response to the stopping powers only from the obtained position-dependent stopping powers with the following assumptions.

(i) The contribution of collective excitation to the position-dependent stopping power depends only on the distance from the surface. We defined it by $\gamma_c(x)$.

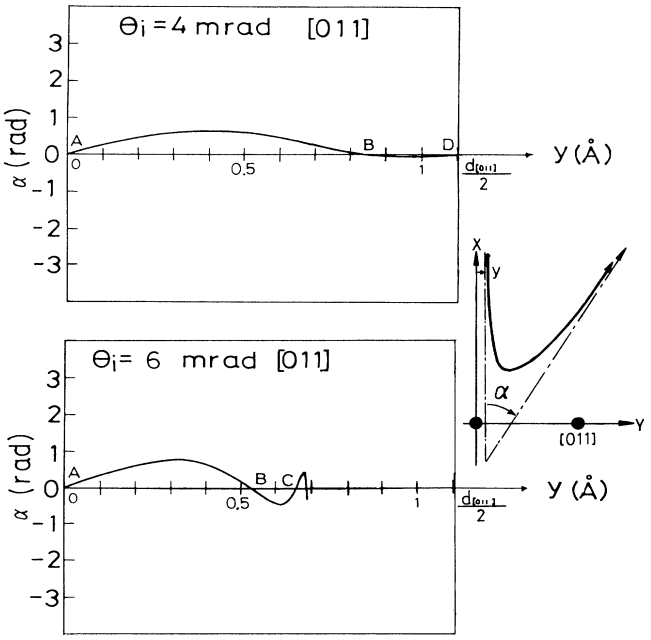

FIG. 6. Examples of the dependence of the angle of scattering relative to the surface plane for the [011] surface-channeled 0.7-MeV He ions on the impact parameter y. The ordinate shows the angle of scattering projected on the scattering plane, (a) at the incidence $\theta_i=4.0$ mrad, and (b) at the incidence $\theta_i=6.0$ mrad.

(ii) Stopping power for surface-channeling ions depends both on x and y. This position-dependent stopping power $S^{[0kl]}(x,y)$ at the $[0kl]$ surface channeling is expressed by

$$S^{[0kl]}(x,y)=\gamma_s^{[0kl]}(x,y)+\gamma_c(x), \tag{7}$$

where $\gamma_s^{(0kl)}(x,y)$ is the contribution of single collisions to the stopping. Since the stopping power $S_a^{[0kl]}(x)$ derived above is obtained for ions with zero impact parameter to the $[0kl]$ atomic rows ($y=0$), it is related to $S^{[0kl]}(x,y)$ by

$$S_a^{[0kl]}(x)=S^{[0kl]}(x,0). \tag{8}$$

Similarly the stopping power $S^{(100)}(x)$ for specular reflection is expressed as

$$S^{(100)}(x)=\gamma_s^{(100)}(x)+\gamma_c(x), \tag{9}$$

where $\gamma_s^{(100)}(x)$ is the contribution of a single collision to $S^{(100)}(x)$.

(iii) We define $\Gamma_s^{[0kl]}(r)$ which shows the contribution of single collisions to the stopping power of an isolated $[0kl]$ atomic row. Thus $\gamma_s^{[0kl]}(x,y)$ and $\gamma_s^{(100)}(x)$ are approximated as

$$\gamma_s^{[0kl]}(x,y)=\sum_{n=-\infty}^{\infty}\Gamma_s^{[0kl]}\{[x^2+(y+na_{[0kl]})^2]^{1/2}\}\ , \quad (10)$$

$$\gamma_s^{(100)}(x)=\frac{1}{a_{[0kl]}}\int_{-\infty}^{\infty}dy\ \Gamma_s^{[0kl]}[(x^2+y^2)^{1/2}]\ . \quad (11)$$

Since type-A trajectory is apart from the neighboring rows, we neglect their effects on $S_a^{[0kl]}(x)$ and retain only the term $n=0$ in $\gamma_s^{[0kl]}(x,0)$ for $S_a^{[0kl]}(x)$. We then obtain an integral equation for $\Gamma_s^{[0kl]}(x)$ from Eqs. (7)–(11),

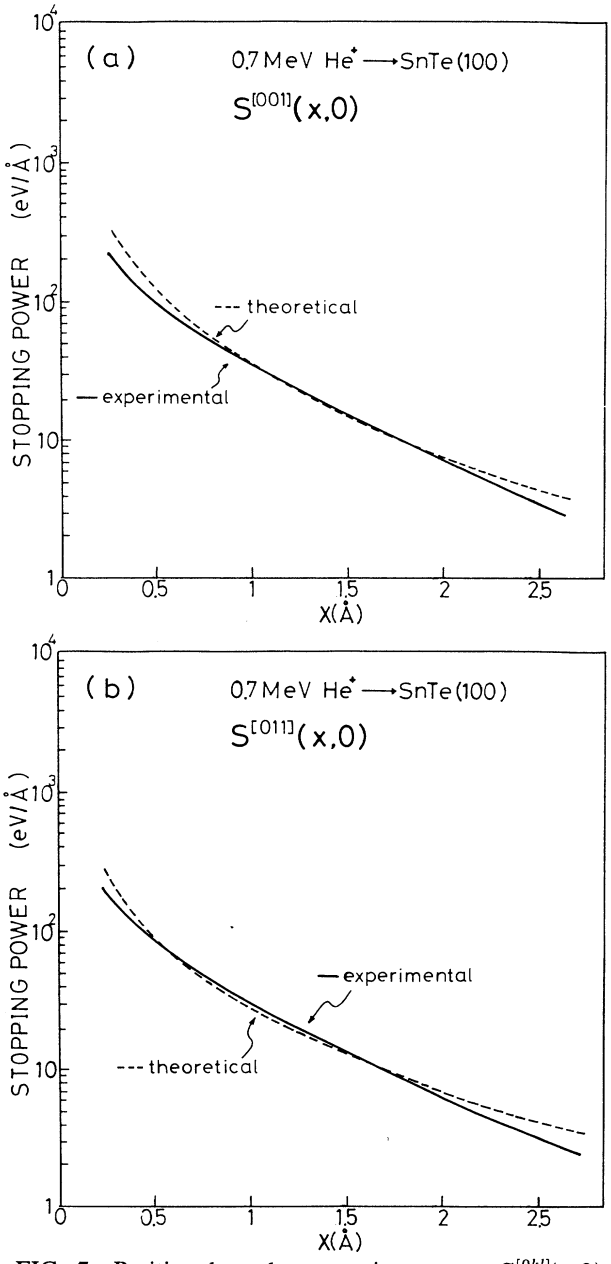

FIG. 7. Position-dependent stopping powers $S_a^{[0kl]}(x,0)$ of the (100) surface for 0.7-MeV He ions. (a) [001] atomic row. (b) [011] atomic row.

$$S^{[0kl]}(x,0)-S^{(100)}(x)=\Gamma_s^{[0kl]}(x)-\frac{1}{a_{[0kl]}}\int_{-\infty}^{\infty}dy\ \Gamma_s^{[0kl]}\{[(x^2+y^2)]^{1/2}\}\ . \quad (12)$$

The left-hand side of Eq. (12) is known from the experimental stopping powers, thus this is again the Abel type integral equation for $\Gamma_s^{[0kl]}(r)$. Equation (12) was solved for the [001] and [011] surface channeling, and $\Gamma_s^{[001]}(r)$ and $\Gamma_s^{[011]}(r)$ were derived. Thus the contribution $\gamma_c(x)$ of collective response of valence electrons to the stopping power was derived from the $\Gamma_s^{[001]}(r)$, $\Gamma_s^{[011]}(r)$, and the observed stopping powers, and is shown in Fig. 8.

We can also derive the position-dependent stopping powers $S^{[001]}(x,y)$ and $S^{[011]}(x,y)$ from Eqs. (7) and (10) with the use of $\Gamma_s^{[001]}(r)$, $\Gamma_s^{[011]}(r)$, and $\gamma_c(x)$ obtained above. The results are shown by contours labeled in eV/Å in Fig. 9. Since the single ion-electron collisions dominate the stopping power near the surface at distances of less than about 1.5 Å, the maxima of the stopping powers are on the atomic rows.

C. Theoretical stopping powers

Effects of collective excitation of surface valence electrons to the stopping power of a metal surface for an ion traveling parallel to the surface have been studied theoretically by many authors [7–11]. The experimental $\gamma_c(x)$ derived above can be compared with the stopping powers calculated from the theories. Here we utilize the formula of the stopping power of an inhomogeneous electron gas, which was derived by Kitagawa under the condition of high-frequency response [11]. The formula of the theoretical stopping power is expressed as

$$\gamma_c(x)=\gamma_b(x)+\gamma_d(x)+\gamma_r(x)\ , \quad (13)$$

$$\gamma_b=\left[\frac{Z_p e\omega_p(x)}{v}\right]^2\ln\frac{2v}{v_F(x)}\ , \quad (14)$$

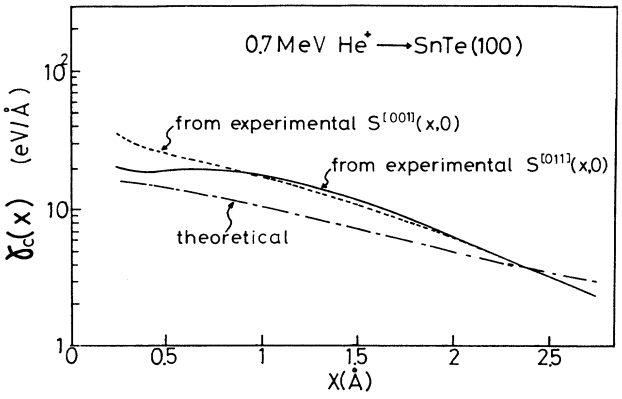

FIG. 8. Contribution of collective response of valence electrons to the stopping power for 0.7-MeV He ion. Experimentally determined $\gamma_c(x)$ from the [001] and [011] surface channeling are compared with the theoretical value $\gamma_c(x)$, where x is the distance from the (100) atomic plane.

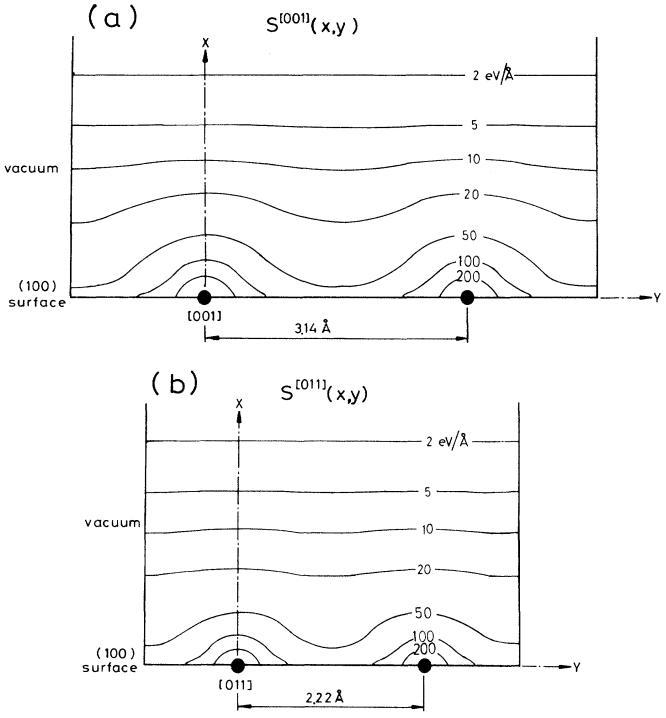

FIG. 9. Position-dependent stopping powers $S^{[0kl]}(x,y)$ of the (100) surface of SnTe (a) at the [001] and (b) at the [011] surface channeling for 0.7-MeV He ions. Atomic rows are shown by the full circles, and the stopping powers are shown by contours labeled in eV/Å.

$$\gamma_d(x)=\int dX\ T_d(X,x)\frac{d\omega_p^2(X)}{2dX}\frac{x-X}{|x-X|}P\frac{1}{\omega_p^2(x)-\omega_p^2(X)}, \tag{15}$$

$$\gamma_r(x)=\int dX\ T_r(X,x)\frac{d\omega_p^2(X)}{2dX}\frac{x-X}{|x-X|}P\frac{1}{\omega_p^2(x)-\omega_p^2(X)}, \tag{16}$$

$$T_d(X,x)=[Z_p e\omega_p(X)/v]^2K_0[2|x-X|\omega_p(X)/v], \tag{17}$$

$$T_r(X,x)=-[Z_p e\omega_p(x)/v]^2K_0[2|x-X|\omega_p(x)/v], \tag{18}$$

$$\omega_p(x)=[4\pi e^2n_v(x)/m]^{1/2},$$

$$v_F(x)=\frac{\hbar}{m}[3\pi^2n_v(x)]^{1/3},$$

where $Z_p e$ is the charge of the ion, $\omega_p(x)$ is the angular frequency of the bulk plasmon of the localized mode, $n_v(x)$ is the density of valence electrons averaged on the yz plane, m is the mass of electron, v is the velocity of ion, and K_0 is the modified Bessel function. Equation (13) was calculated with the valence electron density calculated from the distributions of O-shell electrons of Te and Sn atoms using Hartree-Fock wave functions [12], and with the mean-square charge of the reflected He ions for $(Z_p e)^2$ $(=3.3e^2)$. Since we have no available electron distribution near the (100) surface of SnTe, we used this approximate distribution neglecting the binding of the constituent atoms. The calculated $\gamma_c(x)$ is compared with the experimentally extracted $\gamma_c(x)$ in Fig. 8. Agreement of the calculated and the extracted $\gamma_c(x)$ is good notwithstanding the crude approximation made in deriving $n_v(x)$.

As for the contribution of single collisions to the stopping, $\gamma_s^{[0kl]}(x,y)$, we use a formula based on the binary-encounter approximation [13], which was derived with the use of the method by Lindhard and Scharff [14]. Contribution of the single collisions to the stopping power is expressed,

$$\gamma_s^{[0kl]}(x,y)=\tfrac{1}{2}[Z_p e\omega^{[0kl]}(x,y)/v]^2\ln\left[\frac{2mv^2}{\hbar\omega^{[0kl]}(x,y)}\right], \tag{19}$$

where

$$\omega^{[hkl]}(x,y)=[4\pi e^2n^{[hkl]}(x,y)/m]^{1/2}, \tag{20}$$

where $n^{[0kl]}(x,y)$ is the electron density averaged along the $[0kl]$ axis. Electron-density distribution $n^{[0kl]}(x,y)$ at the (100) surface was calculated with the use of Hartree-Fock wave functions. The calculated $\gamma_s^{[0kl]}(x,0)$ was added to the $\gamma_c(x)$ calculated above, and thus the theoretical stopping powers $S_a^{[0kl]}(x,0)$ for the [001] and [011] surface-channeling He ions were obtained. The results are shown by dashed lines in Fig. 7, which agree well with the observed stopping powers shown by solid lines.

D. Energy spectra of surface-channeled He ions

In order to explain the peaks in the energy spectra of the surface-channeled He ions such as those shown in Figs. 2 and 3, trajectories of He ions were calculated and the stopping power $S^{[0kl]}(x,y)$ was integrated along the four types of trajectories as shown in Fig. 5. As we have expected, the type-A trajectory has the least energy loss, which is approximately 15 kev smaller than the energy of the incident ion. Since the fraction of the ions of a trajectory type is inversely proportional to the gradient of the curve at $\alpha=0$ in Fig. 6, the relative heights of the peaks in an energy spectrum were determined as so. It is not shown in Fig. 6 but the curve crosses the line $\alpha=0$ with larger gradients at several impact parameters larger than the parameter at point C. The ions incident with such impact parameters have longer trajectories in the valleys or near the saddle points of the potential distribution, which result in larger energy losses [15]. Furthermore their fractions are smaller than those of type-A, -B, -C and -D trajectories. Thus they were neglected in the calculation of the spectra.

The calculated energy spectra are shown by bars in Figs. 2 and 3, where the yield of ions of type-A trajectory is normalized to the least energy-loss peak in the observed spectrum except for that in Fig. 3(a). It was not easy to fit the calculated spectra with those obtained experimentally at θ_i smaller than about 3 mrad; an example is shown in Fig. 3(a). Perhaps this may be caused by the experimental uncertainties in θ_i and the detection angle. However, the characteristic features of the observed ener-

gy spectra are well reproduced. This agreement shows that the derived position-dependent stopping powers $S^{[001]}(x,y)$ and $S^{[011]}(x,y)$ and thus the contribution $\gamma_c(x)$ of collective response of valence electrons to the stopping powers are reasonably accurate.

IV. SUMMARY

From the energy spectra of reflected He ions at the [001] and [011] surface channeling of 0.7-MeV He^+ ions on the (100) surface of SnTe single crystal, the position-dependent stopping powers, $S^{[001]}(x,y)$ and $S^{[011]}(x,y)$, of the (100) surface for the [001] and [011] surface-channeling 0.7-MeV He ions were determined. Peak structure of the energy spectra of the He ions reflected from the surface was fairly explained by the stopping powers. Contribution of collective response of valence electrons to the position-dependent stopping powers, $\gamma_c(x)$, was derived the first time from the experimental position-dependent stopping powers. This agreed well with the theories where the dynamical response of valence electrons to the fast-moving ions is taken into account.

ACKNOWLEDGMENT

The authors thank the staff members of the 4-MV Van de Graaff Accelerator of Kyoto University for their assistance in the operation of the accelerator. This work was partly supported by Grant-in-Aid for Scientific Research on Priority Areas "Crystal Growth Mechanism in Atomic Scale" and that for General Scientific Research.

[1] K. Kimura, M. Hasegawa, and M. Mannami, Phys. Rev. B **36**, 7 (1987).
[2] Y. Fujii, K. Narumi, K. Kishine, K. Kimura, and M. Mannami, Nucl. Instrum. Methods B **67**, 82 (1992).
[3] J. Lindhard, K. Dan. Vidensk. Selsk. Mat. -Fys. Medd. **34**, 14 (1965).
[4] D. S. Gemmell, Rev. Mod. Phys. **46**, 129 (1974).
[5] K. Narumi, Y. Fujii, K. Kimura, M. Mannami, and H. Hara, Surf. Sci. (to be published).
[6] Y. Fujii, S. Fujiwara, K. Kimura, and M. Mannami, Nucl. Instrum. Methods B **58**, 18 (1991).
[7] A. A. Lucas, Phys. Rev. B **20**, 4990 (1970).
[8] J. P. Muscat and D. M. Newns, Surf. Sci. **64**, 641 (1977).
[9] R. Nunez, P. M. Echenique, and R. H. Ritchie, J. Phys. C **13**, 4229 (1980).
[10] R. Kawai, N. Itoh, and Y. H. Ohtsuki, Surf. Sci. **114**, 137 (1982).
[11] T. Kitagawa, Nucl. Instrum. Methods B **33**, 409 (1988).
[12] H. Herman and S. Skillman, *Atomic Structure Calculations* (Prentice-Hall, Englewood Cliffs, NJ, 1968).
[13] J. J. Thompson, Philos. Mag. **23**, 419 (1912).
[14] J. Lindhard and M. Scharff, K. Dan. Vidensk. Selsk. Mat. -Fys. Medd. **27**, 15 (1953).
[15] W. Takeuchi and Y. Yamamura, Nucl. Instrum. Methods B **33**, 425 (1988).

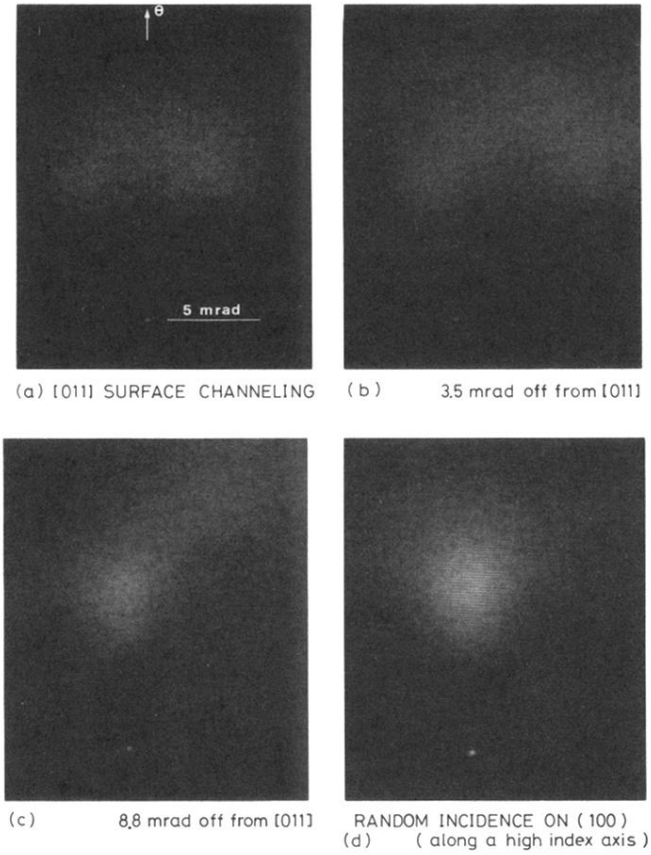

FIG. 1. Angular distributions of scattered He ions at the [011] surface channeling on the (100) surface of SnTe crystal at the incidence of 0.7-MeV He^+ ions. The glancing angle of the incident ions to the (100) surface was 4.8 mrad and the azimuthal angles in the figure were measured from the [011] axis parallel to the (100) surface of SnTe.